OCEAN BASIN REVERBERATION FROM LARGE UNDERWATER EXPLOSIONS
PART 1: SOURCE LEVEL AND PROPAGATION LOSS MODELLING

by

Ira M. Blatstein
Naval Surface Weapons Center, White Oak Laboratory
Silver Spring, Maryland 20910

ABSTRACT

Predicting the reverberant returns from ocean basin reflectors requires describing acoustic source levels for large, conventional underwater explosions, defining the two way propagation loss and signal spreading from the source to the reflector and then to the receiver, and modelling the reflection or scattering process at reflectors such as basin walls. These components must then be put in the framework of a model, or computer program, that relates them properly. This paper will discuss the first two aspects of the problem, namely, the source levels and propagation loss modelling.

Naval Surface Weapons Center, White Oak Laboratory
Silver Spring, Maryland 20910

Following detonation of an underwater explosion, sound reverberates from the ocean surface and bottom and from scatterers within the medium. In addition the boundaries of the ocean basin, and obstructions within it such as sea mounts, reflect the energy incident upon them. Our concern is with these latter signals. In other words, when an explosion is set off in an ocean basin, what particular prominent features of the basin wall and basin interior reflect energy?

As the sound spreads away from the source, its path to the receiver leads to a logical order for discussion of the problem. First one must deal with the definition of the source level or acoustic energy output of the explosion. Then comes examination of propagation to each reflector, the reflection process, and finally propagation to the receiver. This is the order in which Jean Goertner and I will discuss the topic, with Jean showing some comparisons of our model with experimental data.

Probably the most important point that should be emphasized is that simple scattering seems to be sufficient to account for the major aspects of the experimental data that we have examined. In our present model, each five to ten mile section of basin wall-and each sea mount and island-scatters energy very simply as a function of the scattering area and an empirical average scattering strength. The observed arrivals then represent an accumulation of energy from these segments primarily as a function of arrival time, and a reasonable match to the data is achieved. It will be shown that one can further improve the model output by assuming that steep-sloped segments of basin wall scatter more energy than gentle-sloped segments.

The first viewgraph shows two samples of broadband data from underwater explosions that were set off 50 miles apart and approximately ten years apart in the North Atlantic and recorded at Bermuda. In each record, we see a direct arrival from the shock wave itself immediately followed by surface and bottom scattered energy. Further along the record, we see the discrete arrivals from the U. S. East coast, Bahamas, Virgin Islands, etc. that we are interested in. As one might expect, for shots fired in roughly the same location, the reflection patterns are strikingly similar. Thus the overall basin geometry tends to mask whatever sound velocity variability exists in both space and time.

The next two viewgraphs sum up the basic parts of our ocean basin reverberation model. One must start off with a source level model that includes the shock wave plus at least one bubble pulse of the underwater explosion. The model must account for finite amplitude losses out to some range, beyond which acoustic propagation is assumed.

Second one must define a propagation loss model that accounts for geometric spreading and absorption. It must also account for the energy spreading in time that occurs at long ranges due to multipath ray spreading. And finally we have to pick some range at which the close-in spherical spreading changes to long range sound channel propagation with cylindrical spreading.

Next we have to develop a model for the scattering or reflection process. This has to include some depth of interaction so that we can define the basin wall segments along some bottom contour line. It also has to include a scattering area for each segment and a scattering strength common to all segments so that we can compute the energy scattered from each segment. One must determine if basin wall slope, aspect angle, or other parameters significantly affect reflection . Item 4 indicates that all of these elements must be combined in a computer program in order to make predictions.

Returning to item three, we have used the 1000 fathom bottom contour line for defining segments enclosing the North Atlantic basin. The horizontal component for each reflection area is, of course, defined as the length of the segment. The vertical component of each reflection area is assumed to be 1000 fathoms. This leaves item 3c, the average scattering strength, as the empirical constant that must be determined. We did this by finding the value of the scattering strength for which the model output had the same peak reverberation value as one particular case we were treating. We then found, as one hopes in this kind of approach, that the same scattering strength worked equally well for shots of different yields and in other locations in the North Atlantic basin.

I've indicated our approach, and now I would like to briefly discuss source level and propagation loss modeling. The next viewgraph shows the explosion shock wave and bubble pressure time history. Close to the origin, the parameters of this pressure history can be obtained using the well known similitude equations (references 1-3) for shock wave peak pressure, shock wave decay constant, etc. These equations account for the finite amplitude losses incurred by this high amplitude pulse near the source. At some point far enough from the source, the pressure should be low enough that acoustic propagation is applicable for longer ranges. For large explosions, such as the ten ton shots we are treating, this finite amplitude cutoff range may be a considerable distance from the source. But at this range, we should be able to define a pressure history and energy levels using the similitude equations, and then use acoustic propagation-geometric spreading, absorption, etc.-for much longer range propagation.

As shown on the next viewgraph, we start off by first defining the pressure history in a way similar to that used by Weston (reference 4) and closely following work by Weinstein (reference 5). The shock wave is defined as an exponential decay from a peak pressure. The first bubble pulse is defined as a two sided exponential decay with the same time constant in both directions. The negative phase is then specified so that the total impulse is zero. Once P_0, t_0, P_1, t_1, and T_1 are specified, the energy at a given frequency can be found using the transform of the pressure as shown at the bottom of the viewgraph.

Initially we chose 50 nautical miles as our finite amplitude cutoff range. For the ten ton shots we are treating, the shock wave peak pressure is on the order of 1 PSI at this range. We used the similitude equations at a range of 50 nautical miles to find all of the pressure history parameters for the experimental conditions - ten tons of explosive at a depth of 4000 feet. The parameters, such as P_0, t_0, etc. were inserted into the energy expression in order to calculate energy levels over the frequency range of interest. These energy levels were then converted to reference 1 yd source levels for long distance propagation by subtracting out spherical spreading over the 50 nautical mile finite amplitude range.

These levels are shown on the next viewgraph. They are correct at 50 nautical miles if spherical spreading is assumed. And since the pressure is quite low at that range, acoustic propagation can be used for longer distances. Shown in addition to the actual spectrum are third octave band averages. Some of these average values were used in our model calculations in order to match data analysis performed using third octave band filters.

One obvious question is the degree to which the 50 nautical mile finite amplitude cutoff range affects our source level computations. If we use the similitude equations out to a shorter range, we would have lower finite amplitude losses, and therefore higher source levels when referenced back to 1 yd. And similarly, use of the similitude equations to longer ranges would result in higher finite amplitude losses, and lower source levels back at 1 yd. The next viewgraph deals with this quantitatively.

We have done calculations using 10 n.m. and 200 n.m. finite amplitude cutoff ranges. We have done these calculations for our charge weight of interest, ten tons, and one larger weight to see how charge weight enters into the picture. We see that for both yields, when we calculate source levels at 1 yd, the difference in source level for an appreciable change in finite amplitude

cutoff range is only about 3 dB. Thus our source levels are relatively insensitive to the range at which we stop using the similitude equations and start using acoustic propagation-as long as we are an appreciable distance away from the source.

So far, in defining source levels, we have been looking at energy propagating down one ray tube, or along one ray path. Under these circumstances spherical spreading can occur over long ranges. In order to define the total amount of energy reaching a given reflector, one must take into account the focusing of rays back into the sound channel that results from the sound velocity structure. This leads to a transition from spherical spreading close-in to cylindrical spreading at long ranges as many multipaths contribute energy to sound channel axis propagation. The next viewgraph shows a normal mode theory propagation loss calculation for a typical North Atlantic summer profile, a frequency of 50 Hz, a source at 305 meters, and a receiver at the sound channel axis. Also shown on the viewgraph is the simple model we have chosen to use for propagation loss. We have examined similar propagation loss calculations for several oceans of the world, and also determined at what range the bottom grazing ray touches the bottom-leading to a complete ensonification of the sound channel. From this we have chosen 10 nautical miles as the transition range from spherical to cylindrical spreading. This viewgraph and the next one showing loss out to roughly 1000 miles demonstrate that this is a reasonable average propagation loss model for North Atlantic summer conditions. For drastically different profiles, such as the Norwegian Sea profile shown in the next viewgraph, deviations of the simple model from the normal mode calculation of up to 3 dB were observed.

To the propagation loss, we add absorption as a function of frequency. Then relying on work by Ewing and Worzel(reference 6), we assume that the signal spreads approximately one second for every hundred miles of travel, and we spread the total received energy over the indicated period of time for each propagation path.

This talk has dealt with the model in general terms and the source level and propagation model parts in particular. Jean Goertner will now discuss the evolution of the whole reverberation model and show some comparisons with experimental data.

Again simple scattering will be the most important phenomenon with the whole basin defined as a series of small segments each with the same scattering strength. The resulting reverberation versus time is then primarily a simple addition of energy from all of the individual segments around the basin. Obviously, we have a limited set of data, but enough variability so that the model is not tied to one source-receiver geometry. The question, of course, is whether the model is tied to the North Atlantic basin by the average scattering strength or for some other fundamental reason. We hope to answer this question by examining data from other basins in the near future.

Acknowledgement. This work was supported by the Defense Nuclear Agency under subtask V99QAXNH051, "Acoustic Signals." The author would like to acknowledge useful discussions about various aspects of this work with Dr. Marvin Weinstein, Underwater Systems, Inc.

REFERENCES

A. B. Arons, "Underwater Explosion Shock Wave Parameters at Large Distances from the Charge", J. Acoust. Soc. Am. 26 343-346, 1954.

E. A. Christian and M. Black, "Near Surface Measurements of Deep Explosions II. Energy Spectra of Small Charges", J. Acoust. Soc. Am. 38, 57-62, 1965

J. P. Slifko, Pressure Pulse Characteristics of Deep Explosions as a Function of Depth and Range (U) NOLTR 67-87, September 1967 (U)

D. E. Weston, "Underwater Explosions as Acoustic Sources", Proc. Phys. Soc. (London) LXXVI, 2, 233-249 (1960)

M. Weinstein, Underwater Systems Inc., Private Communication

Ewing, M., and J. L. Worzel: Long Range Sound Transmission, Article in "Propagation of Sound in the Ocean", Geological Society of America Memoir 27, 1948.

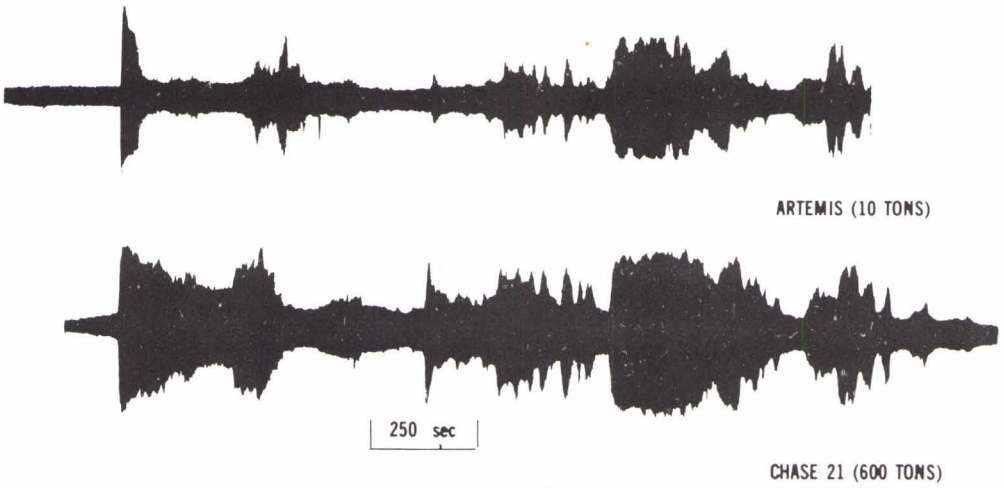

FIG. 1 ARTEMIS 1–2 (10 TONS) AND CHASE 21 (600 TONS) DETONATED IN THE NORTH ATLANTIC AND RECORDED AT BERMUDA

1. SOURCE LEVEL MODEL
   a. SHOCK WAVE PLUS BUBBLE PULSE
   b. FINITE AMPLITUDE EFFECTS
2. PROPAGATION LOSS MODEL
   a. SPREADING LOSS
   b. ABSORPTION
   c. PROPAGATION PATH TIME SPREADING
   d. SPHERICAL/CYLINDRICAL SPREADING TRANSITION RANGE

FIG. 2 OCEAN BASIN REVERBERATION MODEL

3. INTERACTION MODEL FOR REFLECTION PROCESS
   a. DEPTH OF INTERACTION
   b. VERTICAL AND HORIZONTAL REFLECTION REGION
   c. LOSS PER BOUNCE PER UNIT AREA
   d. EFFECT OF WALL SLOPE, ASPECT ANGLE, ETC, ON REFLECTION
   e. TIME SPREADING ON REFLECTION
4. MECHANISM FOR COMBINING MODELS (I.E. COMPUTER PROGRAM)

FIG. 3 OCEAN BASIN REVERBERATION MODEL
Continued

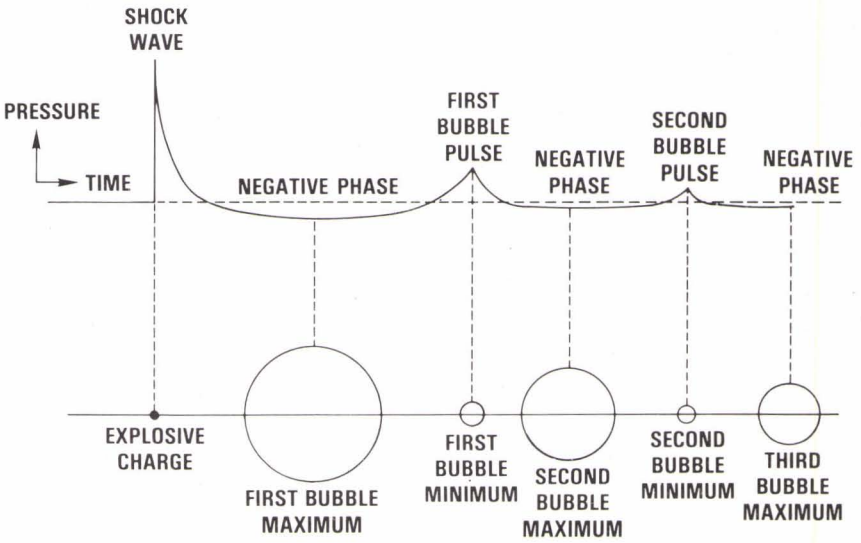

FIG. 4 EXPLOSION BUBBLE AND PRESSURE–TIME HISTORY

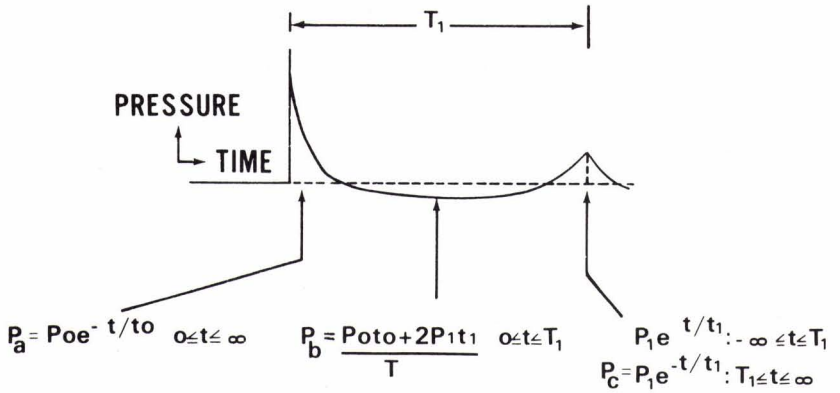

$$E(\omega) = \frac{2}{\rho c}\left\{\left[\frac{Po/to}{1/to^2+\omega^2} + \frac{2\,P_1/t_1}{1/t_1^2+\omega^2}\cos(\omega T_1) - \frac{P_b}{\omega}\sin\omega T_1\right]^2 + \left[\frac{Po\,\omega}{1/to^2+\omega^2} + \frac{2\,P_1/t_1}{1/t_1^2+\omega^2}\sin(\omega T_1) - \frac{P_b}{\omega}(1-\cos(\omega T_1))\right]^2\right\}$$

FIG. 5 SOURCE LEVEL MODEL

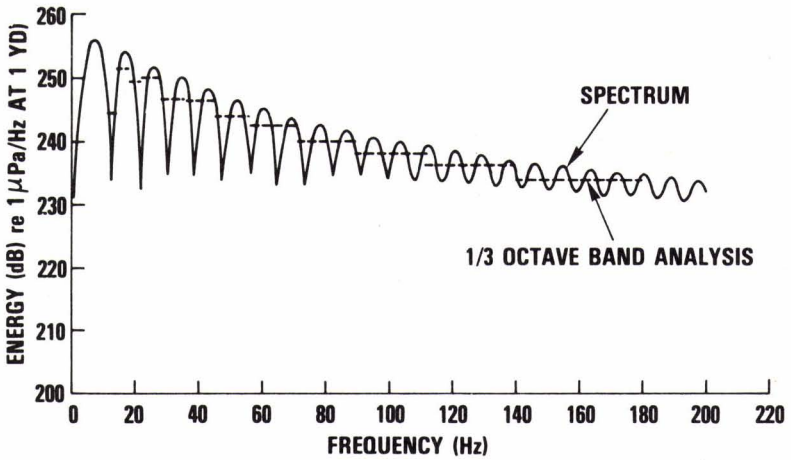

FIG. 6 SOURCE LEVELS
(Charge weight : 20000 lbs, Charge depth : 4000 ft)

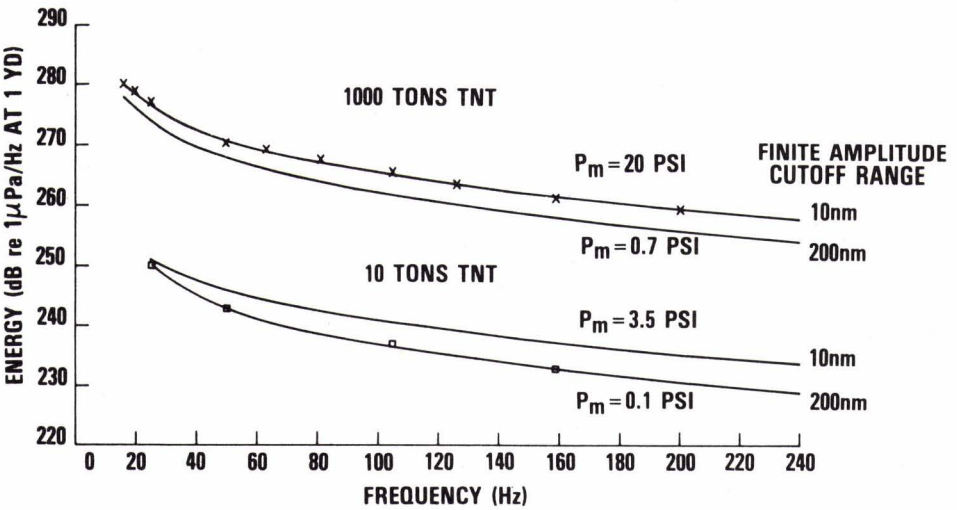

FIG. 7 EFFECT OF FINITE AMPLITUDE CUT-OFF RANGE ON SOURCE LEVEL
(Curves drawn through 1/3 octave band levels at band center)

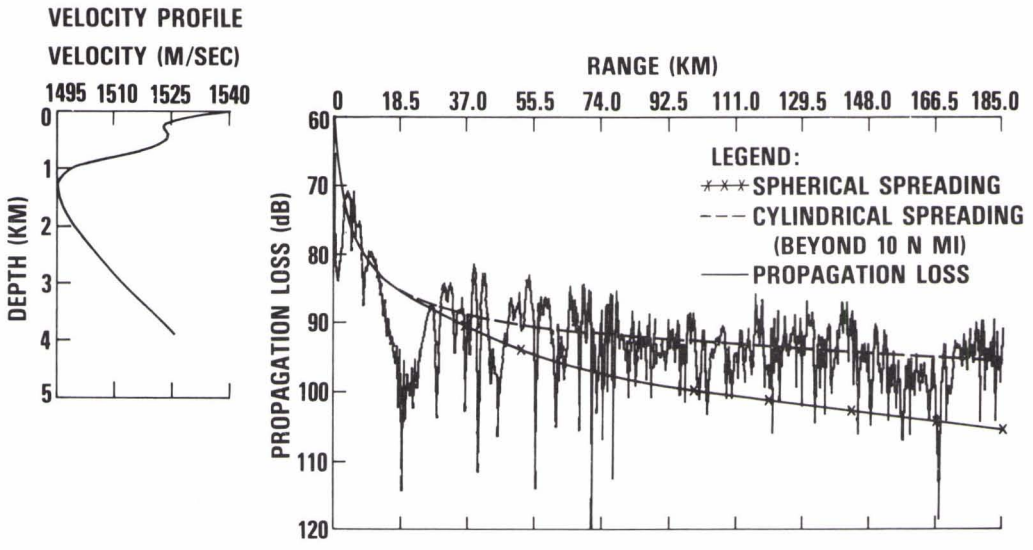

FIG. 8 PROPAGATION LOSS: NORTH ATLANTIC SUMMER
(f = 50 Hz, s = 304.8 M, r = 1188.7 M)

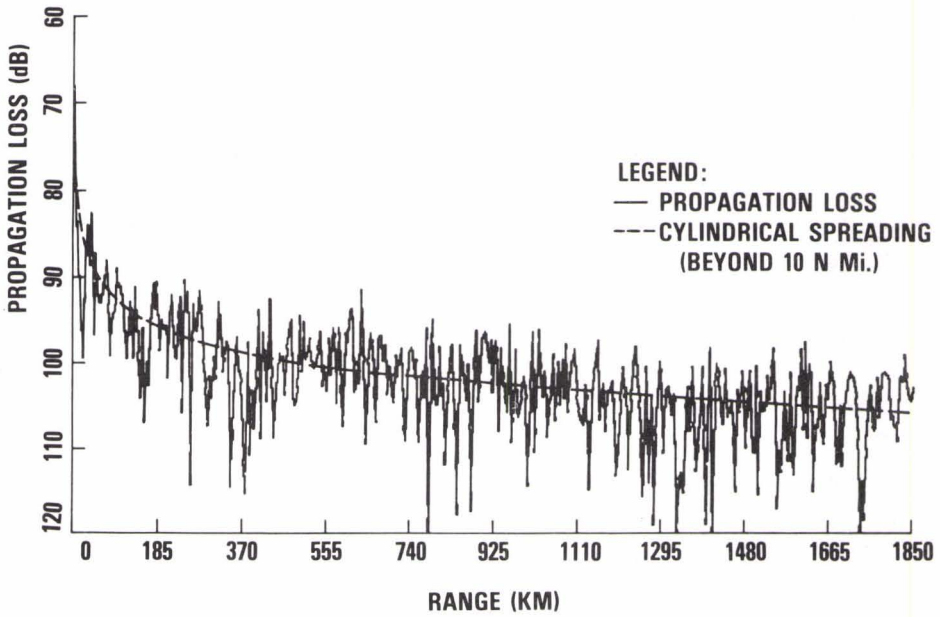

FIG. 9 PROPAGATION LOSS: NORTH ATLANTIC SUMMER
(f = 50 Hz, s = 304.8 M, r = 1188.7 M)

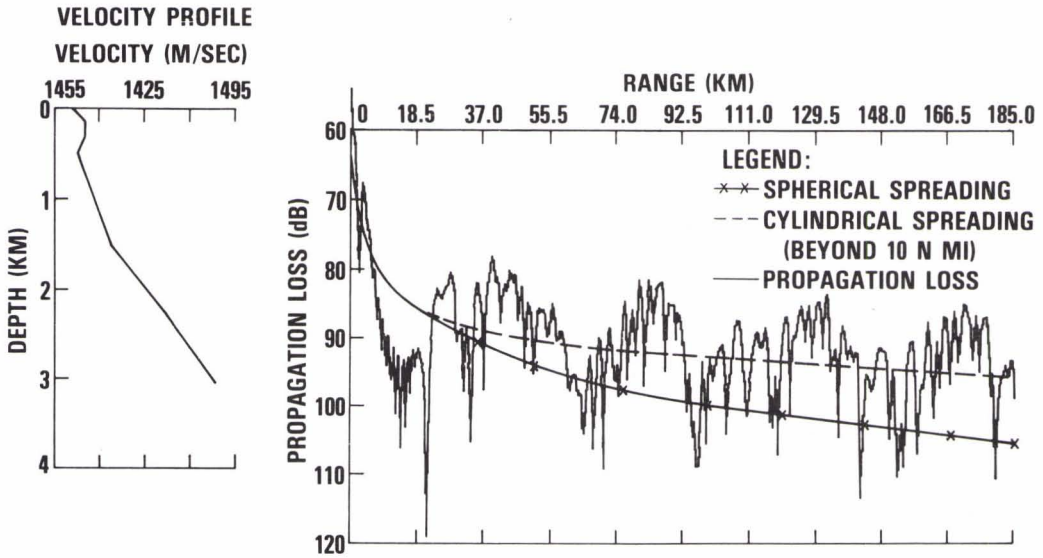

FIG. 10 PROPAGATION LOSS: NORWEGIAN SEA WINTER
(f = 50 Hz, s = 304.8 M, r = 499.8 M)